Title

Controlling the Movement of a TRR Spatial Chain With Coupled Six-Bar Function Generators for Biomimetic Motion

Journal

Journal of Mechanisms and Robotics, 8(5)

ISSN

1942-4302

Authors

Plecnik, Mark M
McCarthy, J Michael

Publication Date

2016-10-01

DOI

10.1115/1.4032105

Peer reviewed

HHS Public Access

Author manuscript

Sci Transl Med. Author manuscript; available in PMC 2016 June 03.

Published in final edited form as:

Sci Transl Med. 2015 June 3; 7(290): 290ra92. doi:10.1126/scitranslmed.3010228.

Drug-induced regeneration in adult mice

Yong Zhang[1,*,†], **Iossif Strehin**[2,*,‡], **Khamilia Bedelbaeva**[1,†], **Dmitri Gourevitch**[1], **Lise Clark**[1], **John Leferovich**[1,§], **Phillip B. Messersmith**[2,¶], and **Ellen Heber-Katz**[1,†,‖]

[1]Molecular and Cellular Oncogenesis Program, The Wistar Institute, Philadelphia, PA 19104, USA.

[2]Department of Biomedical Engineering, Northwestern University, Evanston, IL 60208, USA.

Abstract

Whereas amphibians regenerate lost appendages spontaneously, mammals generally form scars over the injury site through the process of wound repair. The MRL mouse strain is an exception among mammals because it shows a spontaneous regenerative healing trait and so can be used to investigate proregenerative interventions in mammals. We report that hypoxia-inducible factor 1α (HIF-1α) is a central molecule in the process of regeneration in adult MRL mice. The degradation of HIF-1α protein, which occurs under normoxic conditions, is mediated by prolyl hydroxylases (PHDs). We used the drug 1,4-dihydrophenonthrolin-4-one-3-carboxylic acid (1,4-DPCA), a PHD

‖Corresponding author. heberkatz@limr.org.
*These authors are first co-authors.
†Present address: Laboratory of Regenerative Medicine, Lankenau Institute for Medical Research, Wynnewood, PA 19096, USA.
‡Present address: Allergan, Santa Barbara, CA 93111, USA.
§Present address: Department of Pathology and Laboratory Medicine, University of Pennsylvania, Philadelphia, PA 19104, USA.
¶Present address: Bioengineering, Materials Science and Engineering, University of California, Berkeley, Berkeley, CA 94720, USA.

Author contributions: E.H.-K. and P.B.M. designed the studies, analyzed and interpreted results, and wrote the paper. Y.Z. carried out most of the animal experiments and the Western and RT-PCR experiments. I.S. analyzed and carried out drug synthesis, drug crystal synthesis, hydrogel polymer synthesis, drug cytotoxicity studies, and drug release studies. K.B. carried out immunohistochemistry and cell culture studies. D.G. carried out histology and data analysis and prepared the figures. L.C. carried out mouse genetics and phenotyping. J.L. carried out original bioluminescence studies.

SUPPLEMENTARY MATERIALS

www.sciencetranslationalmedicine.org/cgi/content/full/7/290/290ra92/DC1 Materials and Methods
Fig. S1. Knockdown of *Hif1a* in B6 and Swiss Webster mouse ear fibroblasts.
Fig. S2. Effects of Pluronic F127 on microcrystal growth and stability.
Fig. S3. HIF-1α target genes and dedifferentiation marker genes up-regulated by 1,4-DPCA/gel were blocked by knockdown of *Hif1a*.
Fig. S4. HIF-2α is not affected by the 1,4-DPCA drug/gel construct in vitro.
Fig. S5. Distal and long-term effects and survival of drug/gel-treated Swiss Webster mice.
Fig. S6. Inflammatory responses are affected by 1,4-DPCA treatment.
Fig. S7. Synthesis of 1,4-DPCA.
Table S1. Primer sequences used for RT-PCR.
Table S2. Antibodies used for immunostaining.
Table S3. Raw data and statistical significance testing for Fig. 1.
Table S4. Raw data and statistical significance testing for Fig. 3G.
Table S5. Raw data and statistical significance testing for Fig. 4.
Table S6. Raw data and statistical significance testing for Fig. 5.
Table S7. Raw data and statistical significance testing for Fig. 6.
Table S8. Raw data and statistical significance testing for fig. S5.
References (79–82)

Competing interests: A U.S. patent application “Epimorphic regeneration and related hydrogel delivery systems” has been filed in connection with this work (P.B.M., I.S., and E.H.-K.). The other authors declare that they have no competing interests.

Citation: Y. Zhang, I. Strehin, K. Bedelbaeva, D. Gourevitch, L. Clark, J. Leferovich, P. B. Messersmith, E. Heber-Katz, Drug-induced regeneration in adult mice. *Sci. Transl. Med.* **7**, 290ra92 (2015).

inhibitor, to stabilize constitutive expression of HIF-1α protein. A locally injectable hydrogel containing 1,4-DPCA was designed to achieve controlled delivery of the drug over 4 to 10 days. Subcutaneous injection of the 1,4-DPCA/hydrogel into Swiss Webster mice that do not show a regenerative phenotype increased stable expression of HIF-1α protein over 5 days, providing a functional measure of drug release in vivo. Multiple peripheral subcutaneous injections of the 1,4-DPCA/hydrogel over a 10-day period led to regenerative wound healing in Swiss Webster mice after ear hole punch injury. Increased expression of the HIF-1α protein may provide a starting point for future studies on regeneration in mammals.

INTRODUCTION

Wound repair and regeneration are two separate biological processes by which organisms heal wounds (1). There are several models of regeneration in mammals including ear hole closure in rabbits (2, 3), in the inbred mouse strains MRL/MpJ and LG/J (4, 5), and in other mutant mouse strains (6–10). These models show similarities to limb regeneration in amphibians (11, 12) including the replacement of cartilage (4, 13, 14) and the lack of scarring (4, 15, 16). Other less well-known classical regenerative phenotypes, not seen during wound repair, have been observed in the ear injury model of the MRL (Murphy Roths Large) mouse. The MRL mouse is an inbred strain with a genetic background comprising 75% LG (Large) and a 25% mixture of AKR, C3H, and C57BL/6 (4, 5). Regeneration in the MRL mouse includes rapid re-epithelialization, enhanced tissue remodeling, basement membrane breakdown, and blastema growth and redifferentiation (4, 15). Inflammation is now considered a key factor in regenerative processes (17–22). The role of inflammation in ear hole closure has been demonstrated in mice with an acute inflammatory reactivity (AIR) phenotype, which have the ability to close holes made in their ear pinnae (23). A further characteristic of adult MRL mice is their ability to use aerobic glycolysis for normal metabolism, which may contribute to the regenerative response (24). This metabolic state contributes to inflammation, with glycolysis playing an important role in the migration and activity of inflammatory cells (25, 26). The protein hypoxia-inducible factor-1α (HIF-1α) is a central node in all of these processes and could be important in ear hole closure in MRL mice.

HIF-1α is an oxygen-regulated protein that functions as part of a heterodimeric complex, which it forms with HIF-1β in the nucleus. This complex binds to DNA at specific promoter or enhancer sites [hypoxia response elements (HREs)], resulting in transcriptional regulation of more than 100 gene products (27, 28). These include molecules of interest in regenerative processes such as angiogenesis, which is induced by vascular endothelial growth factor (VEGF), VEGF receptor-1 (VEGFR-1), platelet-derived growth factor (PDGF), and erythropoietin (EPO). Other processes involved in regeneration include tissue remodeling, which is induced by urokinase-type plasminogen activator receptor (uPAR), matrix metalloproteinase 2 (MMP2), MMP9, and tissue inhibitors of metalloproteinase (TIMPs), and glycolytic metabolism induced by lactate dehydrogenase (LDH), which converts pyruvate into lactate and pyruvate dehydrogenase kinase (PDK), which blocks the entry of pyruvate into the tricarboxylic acid (TCA) cycle. HIF-1α protein is generally short-lived in the cytoplasm because, under normoxic conditions, it is continually being hydroxylated by

prolyl hydroxylases (PHDs) and then is bound by the von Hippel-Lindau tumor suppressor protein (pVHL) and the recently identified SAG/ROC/RBX2 E3 ubiquitin ligase complex, which targets HIF-1α protein for proteolysis (29). Under low-oxygen conditions, hydroxylation is inhibited, and HIF-1α protein survives and is translocated to the nucleus where it binds to HIF-1β and acts as a transcription factor, binding to the appropriate DNA elements or HREs (30).

The stabilization of HIF-1α protein can be accomplished through inhibition of PHDs, molecules that are also actively involved in collagen secretion and cross-linking. PHDs control collagen deposition in fibrosis, the response to ischemia, and wound repair (31–36). Considering the negative impact of scar formation on regeneration, inhibition of PHDs could have a two-fold effect: stabilization of HIF-1α and down-regulation of scarring. In a chronic diabetic wound repair mouse model, the use of compounds that inhibit PHDs, when applied locally to a wound, can accelerate wound repair in the presence of increased vascularity and granulation tissue that is rich in collagen and other extracellular matrix components (37, 38).

Here, we show that there is increased HIF-1α protein expression in MRL mice after wounding compared to C57BL/6 (B6) mice that do not show a regenerative phenotype. A small interfering RNA (siRNA) against HIF-1α (si*Hif1a*) blocked regeneration in MRL mice after wounding. In another nonregenerative Swiss Webster mouse strain, administering the PHD inhibitor 1,4-DPCA (1,4-dihydrophenonthrolin-4-one-3-carboxylic acid), which stabilizes HIF-1α protein (39, 40), induced regenerative wound healing in these animals.

RESULTS

HIF-1α protein overexpression in MRL mice

After wounding of the ear pinnae of MRL and B6 mice (Fig. 1A), HIF-1α protein expression was measured by immunohistochemistry and Western blot analysis (Fig. 1, B to D and table S3). Higher HIF-1α expression was observed in MRL mouse tissue after injury with peak expression at day 7. For longitudinal studies, HIF-1α reporter mice were created by backcrossing MRL and B6 mice to a transgenic HIF-1α peptide–luciferase reporter mouse [FVB.129S6-Gt(ROSA)26*S*]; the transgene construct used was made by fusing luciferase to the domain of HIF-1α that binds to pVHL in an oxygen-dependent way (41). The MRL. HIF-luc mice showed higher luciferase activity, which was a correlate of HIF-1α protein expression, compared to B6.HIF-luc mice both before injury in the liver and after injury in the ear (Fig. 1, E and F).

Inhibition of ear hole closure in MRL mice by blocking HIF-1α

The requirement for increased HIF-1α protein expression in ear hole closure was demonstrated using *Hif1a* siRNA. Treatment of ear-derived fibroblasts in vitro with a panel of *Hif1a* siRNAs showed that one of four tested siRNAs (si*Hif1a*_3) could completely inhibit constitutive *Hif1a* mRNA expression in MRL fibroblasts (Fig. 1G) and in fibroblasts from B6 and Swiss Webster mice (fig. S1). Next, si*Hif1a*_3 was tested in vivo in MRL.HIF-luc backcross mice for its effect on HIF-1α expression and ear hole closure. Previous studies determined that a hole size of 0 to 0.4 mm in diameter 30 days after injury represented a

regenerative response in MRL mice; a 30-day hole size of 1.2 to 1.6 mm in diameter represented wound repair with scar tissue formation and lack of regeneration in B6 mice (4, 42). Ear hole closure (Fig. 1H and table S3) was blocked by treatment with si*Hif1a*_3 in the MRL.HIF-luc backcross mice (Fig. 1Ha). HIF-1α expression determined by bioluminescence was reduced in MRL reporter mice both in the ear and throughout the body (Fig.1H, b and c).

Stabilization of HIF-1α protein in vitro with a hydrogel loaded with 1,4-DPCA

The compound 1,4-DPCA has been reported to be a potent inhibitor of PHDs and factors inhibiting HIF both in vitro and in vivo. Rats given this compound showed inhibition of collagen hydroxylation and a reduction in collagen deposition (33). By blocking PHDs, 1,4-DPCA stabilizes HIF-1α protein (40) (Fig. 2A). As a delivery system for 1,4-DPCA, we created a polymer hydrogel composed of a cross-linked network of polyethylene glycol molecules that was capable of rapid in situ gel formation from a liquid precursor. This hydrogel system was chosen as the delivery vehicle because of its rapid gelation under physiological conditions, its biocompatibility, and other favorable properties for in vivo use (39). Drug-loaded hydrogels were formed by suspending polymer-stabilized 1,4-DPCA microcrystals in an aqueous mixture of the hydrogel precursors P8Cys and P8NHS (Fig. 2B), which solidified rapidly to entrap the drug microcrystals within the hydrogel (Fig. 2C). In vitro drug release studies demonstrated the delivery of 1,4-DPCA from the hydrogel over several days (Fig. 2, D and E). Because 1,4-DPCA is a poorly soluble drug, crystals were surface-modified with F127 polymer to aid in homogeneous distribution throughout the hydrogel (fig. S2, A and B). Furthermore, entrapment of drug within the hydrogel helped to avoid cytotoxicity observed upon direct contact between cells and drug crystals (fig. S2C).

Fibroblasts from B6 mice cultured with this drug/hydrogel combination (G_d) for 24 hours showed increased expression of HIF-1α, but not HIF-2α, protein in both the cytoplasm and nucleus as determined by immunohistochemistry (Fig. 3A) and Western blot analysis (Fig. 3B) when compared to cells incubated with either gel alone (G_0) or no drug/no gel (Nor.). To determine activation of HIF-1α target gene transcription, we performed reverse transcription polymerase chain reaction (RT-PCR) analysis of mRNA from treated B6 cells. Analysis revealed that the expression of multiple target genes was specifically increased by 1,4-DPCA including the proangiogenic target genes *Vegfa* and *Hmox1* and proglycolytic targets *Ldh-a*, *Pgk1*, *Pdk1*, and *Glut1* (Fig. 3C). Furthermore, the expression of all of these genes was blocked by treatment with si*Hif1a*_3 (fig. S3).

The effect of the 1,4-DPCA drug/hydrogel in vivo in Swiss Webster mice

To test the drug/hydrogel combination in vivo, we used Swiss Webster mice that do not show a regenerative phenotype. An initial attempt to directly apply gel to the ear hole injury site in these mice failed because it could not be maintained on the wound. Thus, the drug/hydrogel was injected subcutaneously at the back of the neck, distal to the wound to attempt to achieve a pharmacological effect. The kinetics of effectiveness of the drug/hydrogel in the injured ear were examined to determine how often reinjection would be necessary. After ear hole punching, a single injection (100 μl) of hydrogel containing drug at either 2 mg/ml (G_d) or 0 mg/ml (gel alone, G_0) was given, and these Swiss Webster mouse groups were

compared to an uninjected group. Ear tissue was harvested daily for 5 days (Fig. 3D). The effect of 1,4-DPCA on HIF-1α protein expression in ear tissue was determined by Western blot analysis (Fig. 3E) and by immunohistochemistry (Fig. 3, F and G and table S4). HIF-1α expression increased on day 1, becoming maximal on days 3 to 4 after injection.

Induction of a regenerative response in Swiss Webster mice by multiple injections of drug/hydrogel

Day 7 after injury was the approximate peak of HIF-1α protein expression in MRL mice, and HIF-1α protein was still elevated in MRL mice on day 14 (Fig. 1D). Therefore, multiple injections of drug/hydrogel were administered to Swiss Webster mice to achieve MRL-like HIF-1α protein expression kinetics. Because a single injection of drug/hydrogel had an effect on HIF-1α expression through day 5, drug/gel or gel alone was injected subcutaneously on days 0, 5, and 10 into three adjacent sites in the back of the neck (Fig. 4A). Complete ear hole closure (Fig. 4, B and C and table S5) was achieved with multiple injections of drug (2 mg/ml)/gel (G_d), with ongoing ear hole closure occurring up to day 35. Furthermore, Western blot analysis (Fig. 4D) showed that although HIF-1α expression was slightly increased in Swiss Webster mice treated with gel alone on day 7 after injury, it was markedly increased in mice treated with drug (2 mg/ml)/gel, similar to what was seen in MRL mice (Fig. 1B). In contrast, HIF-2α expression was barely affected by 1,4-DPCA treatment in the Swiss Webster mice (Fig. 4D), consistent with in vitro experiments (fig. S4). Next, we tested the effects of drug/gel treatment on more distal sites. Mice were injected subcutaneously with drug/gel (on days 0, 5, and 10 after injury) into the left and right rear flank regions (fig. S5A). Only partial ear hole closure (fig. S5B) was achieved at 2 mg/ml, and no closure was observed with drug (1 mg/ml)/gel. We also examined the long-term effects of treatment with drug/gel or gel alone; no histopathological effects or weight changes were seen up to 3 months after treatment (fig. S5C). Finally, Swiss Webster mice were injected three times with drug (2 mg/ml)/gel at the back of the neck and were simultaneously injected with si*Hif1a*_3 every other day for 20 days beginning on day 0 after injury. Ear hole closure induced by 1,4-DPCA/gel on days 14 and 21 was blocked by si*Hif1a* ($P < 0.0001$), indicating that HIF-1α expression induced by the drug/gel contributed to the healing effect (Fig. 4E and table S5).

A potential role for HIF-1α in the regenerative response

We previously showed that the stem cell markers NANOG and SOX2 were up-regulated in regeneration-competent adult MRL mice (24) and that ear-derived fibroblasts from MRL mice in culture displayed multiple stem cell markers not expressed by ear-derived fibroblasts from B6 mice. Fibroblasts from MRL mice (Fig. 5A, first row) stained positive for HIF-1α expression and for a suite of immature cell markers including NANOG. Ear fibroblasts from B6 mice (Fig. 5A, second row) stained negative for HIF-1α expression and immature cell markers, although rare positive staining was seen in dividing cells. However, B6 mouse ear fibroblasts treated in vitro with 1,4-DPCA/gel for 24 hours (Fig. 5A, third row) stained positive for HIF-1α expression as well as for the immature cell markers, displaying both cytoplasmic and nuclear staining that was indistinguishable from that for MRL mouse ear fibroblasts. These results were confirmed by quantitative PCR (qPCR), which showed significant differences between B6 mouse ear fibroblasts treated with

drug/gel versus no gel (Fig. 5B and table S6) ($P_{NANOG} = 0.0004$; $P_{OCT3/4} = 0.0071$). To address the effects of blocking HIF-1α expression on stem cell marker expression, we treated NANOG-positive MRL mouse ear-derived fibroblasts with si*Hif1a* (Fig. 5C); the fibroblasts showed almost complete suppression of NANOG. Similarly, after si*Hif1a* treatment, B6 mouse ear-derived fibroblasts that had been treated with 1,4-DPCA in vitro to induce marker expression showed suppression of these markers (fig. S3).

Very early and rapid re-epithelialization is a feature that distinguishes regeneration from wound repair (43). In the amphibian, reepithelialization is complete within the first 12 hours after injury. Re-epithelialization after ear hole injury in MRL mice occurred between 1 and 2 days after injury, but not until as late as 5 to 10 days after injury in the nonregenerating B6 and other mouse strains (4, 16). Swiss Webster mice treated with drug/gel showed re-epithelialization by day 2 after injury, in contrast to mice treated with gel only (Fig. 6A, a and b). HIF-1α expression in Swiss Webster mouse ear epidermis was seen on day 1, followed by WNT5a expression on day 2 (Fig. 6A, c to f), similar to what was observed in drug-treated ear-derived fibroblasts in vitro (Fig. 6A, g to i). Paralleling the response in vitro (Fig. 5A), cellular dedifferentiation was also seen in vivo after a single injection of 1,4-DPCA drug/gel into Swiss Webster mice (Fig. 6B, a and b). Expression of the stem cell markers NESTIN, OCT3/4, neurofilament, and PAX7 was detected by immunohistochemistry (Fig. 6B, c to f) and qPCR (Fig. 6Bg) and peaked at days 4 to 5 after injury in Swiss Webster mice receiving the drug/gel.

Expression of laminin, a major component of the basement membrane, was reduced in Swiss Webster mouse ear tissue after 1,4-DPCA/gel treatment (Fig. 6C, a and b), and laminin expression was absent from the epithelial-mesenchymal border. Expression of MMP9, a major protease involved in laminin breakdown, increased after drug treatment (Fig. 6Cc), along with markers for inflammatory cells that have been associated with tissue remodeling, such as the neutrophil markers myeloperoxidase (MPO) and Ly6G (Fig. 6C, d and e) and mast cell markers (fig. S6). Next, we examined scar formation after drug/gel treatment of Swiss Webster mice using staining with picrosirius red (a marker of collagen cross-linking). Scar formation was reduced after drug/gel treatment but was restored after treatment of the mice with si*Hif1a* (Fig. 6D, a to d and table S7). In addition to reduced PHD function after 1,4-DPCA/gel treatment, the expression of lysyl oxidase–like 4 (*Loxl4*) and connective tissue growth factor (*Ctgf*), elements of scar tissue formation, was also reduced by drug/gel treatment as shown by qPCR in ear tissue from Swiss Webster mice (Fig. 6De).

Finally, blastema growth and redifferentiation including chondrogenesis and hair follicle growth, which are generally considered later events in the regenerative process, were also affected by 1,4-DPCA/gel treatment. A major difference in ear hole size with accompanying chondrogenesis and appearance of hair follicles (Fig. 6E, a to h and table S7) was apparent by day 35 after drug/gel treatment of Swiss Webster mice. Differences in inward tissue growth were seen (Fig. 6Ec) as well as changes at the end of the cartilage at the site of the original punch margin (Fig. 6E, e to h and table S7), which showed new chondrogenesis. Furthermore, expression of the chondrogenesis-associated genes *Mgp*, *Itm2a*, *Matn3*, *Mia2*, *Col11a1*, *Prg4*, *Fmod*, and *Chad* was up-regulated on day 21 after injury in Swiss Webster mice treated with drug/gel (Fig. 6Ed and table S7). In addition, hair follicles expressing

keratin 14 were found in ear tissue from drug/gel-treated but not in ear tissue from gel only–treated mice, with keratin 14 expression similar to that found for normal ear tissue (Fig. 6E, j and k and table S7). Expression of the genes *S100a4*, *Wif1*, *Dkk3*, *Dcn*, and *Tgfb2* in the growing hair follicle bulge region was also increased in drug/gel-treated but not in gel-treated Swiss Webster mice (Fig. 6Ei and table S7).

DISCUSSION

Following its discovery (27), there has been a growing recognition that HIF-1α is a master regulator of cellular processes including regulation of oxygen concentrations, aerobic glycolysis, cell migration, and inflammation. Our study suggests that another role for HIF-1α is in mammalian tissue regeneration. Given the role of HIF-1α in cellular processes that distinguish tissue regeneration from scar formation, we explored the role of HIF-1α in regenerative wound healing in the MRL mouse. The MRL mouse strain uses aerobic glycolysis as its basal metabolic state (24) and is able to regenerate many tissue types after injury. Furthermore, a recent genetic mapping study shows that RNF7, an E3 ligase necessary for HIF-1α ubiquitination, is associated with ear hole regeneration in LG/J mice. Expression of *Rnf7* is down-regulated in both MRL and LG/J mice (an MRL mouse parental strain contributing 75% of the MRL genome), resulting in a predicted increase in HIF-1α expression (44). Here, we show that HIF-1α is up-regulated in unwounded MRL mice compared to B6 and Swiss Webster mice. Expression of HIF-1α was further increased in MRL mice after wounding (ear hole punching). Treatment of MRL mice after injury with si*Hif1a*, which blocked HIF-1α expression, inhibited ear hole closure. To determine the effects of increased HIF-1α expression in Swiss Webster mice that do not have a regenerative phenotype, we subcutaneously injected these animals with the HIF-1α–stabilizing drug 1,4-DPCA in a hydrogel (39). Administering the drug/gel subcutaneously both proximal and distal to the ear wound sites resulted in accelerated ear hole closure. As in MRL mice, si*Hif1a* treatment blocked this drug-induced regenerative response, supporting the notion that up-regulation of HIF-1α in mice is sufficient to lead to a regenerative response in ear pinnae after wounding.

Formulating the 1,4-DPCA drug in a hydrogel enabled slow delivery of the drug over 4 to 10 days, depending on the gel formulation and drug dose. Treatment of mice with the drug/gel increased HIF-1α protein expression for up to 5 days. Trapping microcrystals of the drug within a hydrogel avoided potential cytotoxicity associated with direct uptake of drug crystals by cells. In terms of specificity, 1,4-DPCA interacted with and blocked PHD function and increased HIF-1α expression. We showed that the drug did not affect the expression of HIF-2α (also regulated by PHDs) in either fibroblasts or endothelial cells (fig. S4) and that HIF-2α expression was not affected in ear tissue after drug/gel treatment.

Central to limb regeneration in amphibians is the blastema. The blastema is a tissue structure seen in the developing embryo and in regenerating tissue that is made up of a mass of undifferentiated pluripotent cells that can proliferate and then produce a copy of the lost structure (12, 45). The process starts with rapid coverage of the wound by epithelial cells (re-epithelialization), which occurs in the absence of a basement membrane potentially due to increased MMP protease activity (46, 47). Reforming the basement membrane in

regenerating amphibian limbs after retinoic acid treatment leads to scarring and lack of blastema growth (48, 49). In the next step of blastema growth, nondividing mesenchymal cells migrate under the new epidermis as the accumulation blastema and then divide, resulting in tissue elongation and expansion; the cells finally redifferentiate into the lost appendage (50).

HIF-1α–regulated ear hole closure in MRL mice and drug-treated Swiss Webster mice appears to go through a process that has some of the hallmarks of the blastema and its formation. HIF-1α is most highly expressed in the early phase of the regenerative response in which cells are migratory, nonproliferative, and dedifferentiated. This is consistent with up-regulation of molecules such as WNT5a, involved in cell migration (51–53), and NANOG and OCT3/4, which are markers of pluripotent stem cells, oocytes, and the early embryo (54, 55). Development of the embryo occurs under low-oxygen conditions, resulting in increased expression of HIF-1α, morphogenesis (56), and increased stem cell marker expression (57, 58).

MRL mouse ear tissue showed unusual expression of a range of diverse stem cell markers both in vitro and in vivo, including NANOG, SOX2, OCT3/4, CD34, and CD133. NESTIN is a neuronal stem and progenitor cell marker, PAX7 is a satellite muscle-associated stem cell marker, WNT5a is an early marker involved in migration, and PREF1 or DLK1 is a preadipocyte/hepatocyte stem cell marker. Expression of these molecules was not observed in ear tissue of B6 or Swiss Webster mice. HIF-1α stabilization by the drug 1,4-DPCA led to an increase in expression of all of these differentiation markers in Swiss Webster and B6 mouse fibroblasts, although only transiently. Treatment with si*Hif1a* blocked NANOG expression in MRL mouse ear fibroblasts, suggesting that the expression of this marker is due to increased HIF-1α. In addition to a hypoxic environment and elevated HIF-1α, pluripotent embryonic stem cells maintain a glycolytic metabolic state (59). Adult quiescent mesenchymal and hematopoietic stem cells also may utilize glycolytic metabolism (59, 60) like in adult MRL mice (24), other animal models of regeneration (61, 62), and some examples of surgical wounds (63). Surprisingly, HIF-2α expression, reported to modulate expression of NANOG and OCT3/4 (64), does not increase during ear hole closure; however, a recent study shows that other factors such as miR-302 can also regulate expression of OCT3/4 (65).

HIF-1α regulates MMPs, which in turn degrade extracellular matrix including laminin and basement membrane remodeling proteins. Like MRL mice (15, 16), Swiss Webster mice treated with the drug 1,4-DPCA (a PHD inhibitor) show increased MMP9 expression and a vanishing basement membrane (Fig. 6C, a and b). A second regeneration-promoting effect of 1,4-DPCA is collagen hydroxylation, leading to reduced scarring and increased collagen degradation (33, 40, 66, 67). MRL mice and 1,4-DPCA–treated Swiss Webster mice also show reduced expression of scar-associated markers *Loxl4* and *Ctgf* (17, 68); in contrast, hypoxia-induced remodeling molecules are increased, including lysyl oxidase (69) and collagen prolyl (P4HA1,2) and lysyl (PLOD2) hydroxylases. These molecules are also regulated by HIF-1α and result in increased extracellular matrix stiffness and alignment (70), indicating that hypoxia may mediate tissue component structure beyond a specific HIF-1α effect (see fig. S4).

In MRL mice, elastic and articular cartilage formation begins at about 1 month after injury and can be fully regenerated by 3 to 4 months after injury (13, 14). With 1,4-DPCA treatment of Swiss Webster mice after ear hole punch injury, the new growth area shows chondrogenesis by day 35, with up-regulation of multiple chondrogenesis markers including those found in chondrogenic precursor cells (71–74) and in cartilage extracellular matrix (75, 76). Hair follicle formation was also found in the new growth area at a level seen in normal tissue, and multiple markers of bulge-derived keratinocyte stem cells (77) and epithelial sac cells involved in regeneration were also expressed in drug-treated Swiss Webster mice (78). Together, our data demonstrate that spontaneous regeneration in MRL mice with ear hole punch injury can be mimicked in nonregenerating Swiss Webster mice by treatment with the drug 1,4-DPCA/hydrogel, which stabilizes HIF-1α, indicating that HIF-1α is a regulator of mammalian regeneration in vivo. However, a key limitation of this study is that it remains untested whether modulating HIF-1α expression in other mammals and in humans will induce a regenerative healing response to wounds. Finally, whereas the ear hole punch model has proven to be a reliable proxy for wound healing studies in multiple tissues in regenerating and nonregenerating mice, future HIF-1α modulation studies will be required to generalize these findings to other tissue injury sites.

MATERIALS AND METHODS

Study design

We used inbred mouse strains to study the effect of a small-molecule inhibitor of PHDs on the in vitro and in vivo expression of HIF-1α and the impact on quantitative regenerative ear hole closure (4, 42). In animal studies, 2.1-mm ear hole punch wounds were created in ear pinnae, and a 1,4-DPCA–containing hydrogel was subcutaneously implanted in the back of the neck of the wounded mice at multiple time points. Healing was monitored by measuring hole diameters. End points of the study were previously determined to be 30+ days after injury (4, 15, 24, 42) and included key indices of tissue regeneration such as blastema formation and epithelial, dermal, and cartilaginous wound closure with hair follicle replacement plus expression of multiple molecular markers of cellular dedifferentiation, redifferentiation, and stem cell state. These parameters were determined by physical measurements of wound closure, standard tissue histology and histomorphometry, and gene expression using quantitative immunohistochemistry, Western blot analysis, and qPCR. The experimental groups were coded, and different laboratory personnel were involved in doing ear wounding, injections, phenotyping, and data analysis.

Animals and in vivo procedures

MRL/MpJ and HIF-1α::ODD-luciferase reporter [FVB.129S6-Gt(ROSA)26Sortm2(HIF1A/luc)Kael/J] mice were obtained from The Jackson Laboratory; C57BL/6 mice were from Taconic Laboratories; Swiss Webster mice were from Charles River. Mice were used at about 8 to 10 weeks of age in all experiments under standard conditions at the Wistar Institute Animal Facility, and the protocols were in accordance with the National Institutes of Health (NIH) *Guide for the Care and Use of Laboratory Animals*. Through-and-through ear hole punches were carried out as previously described (4), and each ear hole diameter was measured in the direction of the ear pinna long axis and then the perpendicular axis.

IVIS luciferase scanning

To detect luciferase expression in vivo, mice were given a single intraperitoneal injection of D-luciferin (37.5 mg/kg, Gold Biotechnology Inc.) in sterile water. Fifteen minutes later, mice were anesthetized using isoflurane and placed in a light-tight chamber equipped with a charge-coupled device IVIS imaging camera (Xenogen). Photons were collected for a period of 1 to 5 min, and images were obtained by using Living Image software (Xenogen) and IGOR image analysis software (WaveMetrics). HIF-1α ODD luc expression after ear punching was determined in MRL and B6 mice backcrossed to the transgenic HIF-1α peptide–luciferase reporter mouse FVB.129S6-Gt(ROSA)26*S*, made by fusing luciferase to the domain of HIF-1α that binds to pVHL in an oxygen-dependent way (ODD peptide) and selected for luciferase positivity.

Hif1a siRNA transfection in vitro and in vivo

B6, Swiss Webster, and MRL mouse ear fibroblast-like cells at 70% of confluence were transfected with 100 nM of four different *Hif1a* siRNAs (SI00193025, SI00193032, Sl00193011, and SI00193018; purchased from Qiagen) and scramble siRNA (sc-37007, Santa Cruz Biotechnology), using Lipofectamine 2000 according to the manufacturer's protocol. Transfected cells were examined for knockdown efficiency after 48 hours of transfection. siRNA Mm_*Hif1a*_3 (SI00193025) was selected for the in vitro experiments because of its high efficiency. In vivo, siRNA Mm_*Hif1a*_3 was used for HIF-1α inhibition. Si*Hif* at 75 mg/kg was mixed with Jetpei (Polyplus, Genycell) following the manufacturer's instructions and was then injected into animals subcutaneously every 48 hours.

In vivo hydrogel injection

Swiss Webster mice were injected subcutaneously at the base of the neck with 100 μl of 10% (w/v) 1:1 (w/w) ratio of P8Cys (with or without 1,4-DPCA drug crystal) to P8NHS hydrogel prepared in PBS (Fig. 2B and Supplementary Materials). Each component was kept cold and mixed just before injection. At different time points, mice were euthanized and tissues were removed for protein and RNA analysis.

Statistical analysis

All experiments were repeated multiple times (*N*). The data represent pooled samples for Western blot analysis and qPCR, and individual samples in healing studies and tissue analysis (*n*) as indicated in the figure legends. All experiments used inbred mouse strains reducing individual-to-individual variation. Student's *t* test was carried out to compare differences of means from independent samples between two groups. The ANOVA test was performed to determine if there were significant differences among the means of more than two groups. If the *P* value from ANOVA analysis was significant, then the post hoc Tukey test was applied to compare the mean between each group. *P* values ≤0.05 were considered significant, and *P* values ≤0.01 were considered highly significant. All error bars shown on the graphs represent SEs, except in Fig. 2 where SD is used. The software used for the ANOVA analysis and the post hoc Tukey test is R version 2.14.1. All other statistical analyses were done using Microsoft Excel 2010.

Supplementary Material

Refer to Web version on PubMed Central for supplementary material.

Acknowledgments

We thank X. Yin, Q. Liu, R. Davulari, Y. Bi, and A. Weeraratna for useful discussions and statistical advice, and M. O'Connell and A. Weeraratna for providing reagents.

Funding: Supported, in whole or in part, by NIH grants from the National Institute of Dental and Craniofacial Research, RO1 DE021215 and DE021104, with other funding from the F. M. Kirby Foundation and the G. Harold and Leila Y. Mathers Foundation. These studies used the Wistar Institute Animal Facilities, Histotechnology Facility, and Research Supplies Facility, which are supported by a Wistar Cancer Center grant from the National Cancer Institute, NIH (P30 CA010815).

REFERENCES AND NOTES

1. Kawasumi A, Sagawa N, Hayashi S, Yokoyama H, Tamura K. Wound healing in mammals and amphibians: Toward limb regeneration in mammals. Curr. Top. Microbiol. Immunol. 2013; 367:33–49. [PubMed: 23263248]
2. Joseph J, Dyson M. Tissue replacement in the rabbit's ear. Br. J. Surg. 1966; 53:372–380. [PubMed: 5931030]
3. Goss RJ, Grimes LN. Tissue interactions in regeneration of rabbit ear holes. Am. Zool. 1972; 12:151–157.
4. Clark LD, Clark RK, Heber-Katz E. A new murine model for mammalian wound repair and regeneration. Clin. Immunol. Immunopathol. 1998; 88:35–45. [PubMed: 9683548]
5. Kench JA, Russell DM, Fadok VA, Young SK, Worthen GS, Jones-Carson J, Henson JE, Nemazee D. Aberrant wound healing and TGF-β production in the autoimmune-prone MRL/+ mouse. Clin. Immunol. 1999; 92:300–310. [PubMed: 10479535]
6. Bedelbaeva K, Snyder A, Gourevitch D, Clark L, Zhang XM, Leferovich J, Cheverud JM, Lieberman P, Heber-Katz E. Lack of p21 expression links cell cycle control and appendage regeneration in mice. Proc. Natl. Acad. Sci. U.S.A. 2010; 107:5845–5850. [PubMed: 20231440]
7. Liu J, Johnson K, Li J, Piamonte V, Steffy BM, Hsieh MH, Ng N, Zhang J, Walker JR, Ding S, Muneoka K, Wu X, Glynne R, Schultz PG. Regenerative phenotype in mice with a point mutation in transforming growth factor β type I receptor (TGFBR1). Proc. Natl. Acad. Sci. U.S.A. 2011; 108:14560–14565. [PubMed: 21841138]
8. Oike Y, Yasunaga K, Ito Y, Matsumoto S, Maekawa H, Morisada T, Arai F, Nakagata N, Takeya M, Masuho Y, Suda T. Angiopoietin-related growth factor (AGF) promotes epidermal proliferation, remodeling, and regeneration. Proc. Natl. Acad. Sci. U.S.A. 2003; 100:9494–9499. [PubMed: 12871997]
9. Cho CH, Sung HK, Kim KT, Cheon HG, Oh GT, Hong HJ, Yoo OJ, Koh GY. COMP-angiopoietin-1 promotes wound healing through enhanced angiogenesis, lymphangiogenesis, and blood flow in a diabetic mouse model. Proc. Natl. Acad. Sci. U.S.A. 2006; 103:4946–4951. [PubMed: 16543381]
10. Shyh-Chang N, Zhu H, Yvanka de Soysa T, Shinoda G, Seligson MT, Tsanov KM, Nguyen L, Asara JM, Cantley LC, Daley GQ. Lin28 enhances tissue repair by reprogramming cellular metabolism. Cell. 2013; 155:778–792. [PubMed: 24209617]
11. Heber-Katz E, Zhang Y, Bedelbaeva K, Song F, Chen X, Stocum DL. Cell cycle regulation and regeneration. Curr. Top. Microbiol. Immunol. 2013; 367:253–276. [PubMed: 23263201]
12. Brockes JP, Kumar A. Comparative aspects of animal regeneration. Annu. Rev. Cell Dev. Biol. 2008; 24:525–549. [PubMed: 18598212]
13. Fitzgerald J, Rich C, Burkhardt D, Allen J, Herzka AS, Little CB. Evidence for articular cartilage regeneration in MRL/MpJ mice. Osteoarthritis Cartilage. 2008; 16:1319–1326. [PubMed: 18455447]

14. Rai MF, Hashimoto S, Johnson EE, Janiszak KL, Fitzgerald J, Heber-Katz E, Cheverud JM, Sandell LJ. Heritability of articular cartilage regeneration and its association with ear wound healing in mice. Arthritis Rheum. 2012; 64:2300–2310. [PubMed: 22275233]
15. Gourevitch D, Clark L, Chen P, Seitz A, Samulewicz SJ, Heber-Katz E. Matrix metalloproteinase activity correlates with blastema formation in the regenerating MRL mouse ear hole model. Dev. Dyn. 2003; 226:377–387. [PubMed: 12557216]
16. Gourevitch DL, Clark L, Bedelbaeva K, Leferovich J, Heber-Katz E. Dynamic changes after murine digit amputation: The MRL mouse digit shows waves of tissue remodeling, growth, and apoptosis. Wound Repair Regen. 2009; 17:447–455. [PubMed: 19660054]
17. Gourevitch D, Kossenkov AV, Zhang Y, Clark L, Chang C, Showe LC, Heber-Katz E. Inflammation and its correlates in regenerative wound healing: An alternate perspective. Adv. Wound Care. 2014; 3:592–603.
18. Yin Y, Henzl MT, Lorber B, Nakazawa T, Thomas TT, Jiang F, Langer R, Benowitz LI. Oncomodulin is a macrophage-derived signal for axon regeneration in retinal ganglion cells. Nat. Neurosci. 2006; 9:843–852. [PubMed: 16699509]
19. Wada K, Arita M, Nakajima A, Katayama K, Kudo C, Kamisaki Y, Serhan CN. Leukotriene B_4 and lipoxin A_4 are regulatory signals for neural stem cell proliferation and differentiation. FASEB J. 2006; 20:1785–1792. [PubMed: 16940150]
20. Kyritsis N, Kizil C, Zocher S, Kroehne V, Kaslin J, Freudenreich D, Iltzsche A, Brand M. Acute inflammation initiates the regenerative response in the adult zebrafish brain. Science. 2012; 338:1353–1356. [PubMed: 23138980]
21. Goh YP, Henderson NC, Heredia JE, Red Eagle A, Odegaard JI, Lehwald N, Nguyen KD, Sheppard D, Mukundan L, Locksley RM, Chawla A. Eosinophils secrete IL-4 to facilitate liver regeneration. Proc. Natl. Acad. Sci. U.S.A. 2013; 110:9914–9919. [PubMed: 23716700]
22. Kalish BT, Kieran MW, Puder M, Panigrahy D. The growing role of eicosanoids in tissue regeneration, repair, and wound healing. Prostaglandins Other Lipid Mediat. 2013; 104–105:130–138.
23. De Franco M, Carneiro Pdos S, Peters LC, Vorraro F, Borrego A, Ribeiro OG, Starobinas N, Cabrera WK, Ibanez OM. *Slc11a1* (*Nramp1*) alleles interact with acute inflammation loci to modulate wound-healing traits in mice. Mamm. Genome. 2007; 18:263–269. [PubMed: 17486412]
24. Naviaux RK, Le TP, Bedelbaeva K, Leferovich J, Gourevitch D, Sachadyn P, Zhang XM, Clark L, Heber-Katz E. Retained features of embryonic metabolism in the adult MRL mouse. Mol. Genet. Metab. 2009; 96:133–144. [PubMed: 19131261]
25. O'Neill LA, Hardie DG. Metabolism of inflammation limited by AMPK and pseudo-starvation. Nature. 2013; 493:346–355. [PubMed: 23325217]
26. Nathan C. Immunology: Oxygen and the inflammatory cell. Nature. 2003; 422:675–676. [PubMed: 12700748]
27. Semenza GL. HIF-1 and mechanisms of hypoxia sensing. Curr. Opin. Cell Biol. 2001; 13:167–171. [PubMed: 11248550]
28. Weidemann A, Johnson RS. Biology of HIF-1α. Cell Death Differ. 2008; 15:621–627. [PubMed: 18259201]
29. Tan M, Gu Q, He H, Pamarthy D, Semenza GL, Sun Y. SAG/ROC2/RBX2 is a HIF-1 target gene that promotes HIF-1α ubiquitination and degradation. Oncogene. 2008; 27:1404–1411. [PubMed: 17828303]
30. Wenger RH, Stiehl DP, Camenisch G. Integration of oxygen signaling at the consensus HRE. Sci. STKE. 2005; 2005:re12. [PubMed: 16234508]
31. Liu XH, Kirschenbaum A, Yao S, Stearns ME, Holland JF, Claffey K, Levine AC. Up-regulation of vascular endothelial growth factor by cobalt chloride-simulated hypoxia is mediated by persistent induction of cyclooxygenase-2 in a metastatic human prostate cancer cell line. Clin. Exp. Metastasis. 1999; 17:687–694. [PubMed: 10919714]
32. Zhang XJ, Liu LX, Wei XF, Tan YS, Tong L, Chang R, Marti G, Reinblatt M, Harmon JW, Semenza GL. Importance of hypoxia-inducible factor 1α in healing of burn wounds in a murine model. Wound Repair Regen. 2009; 17:A87.

33. Franklin TJ, Morris WP, Edwards PN, Large MS, Stephenson R. Inhibition of prolyl 4-hydroxylase in vitro and in vivo by members of a novel series of phenanthrolinones. Biochem. J. 2001; 353:333–338. [PubMed: 11139398]
34. Hill P, Shukla D, Tran MGB, Aragones J, Cook HT, Carmeliet P, Maxwell PH. Inhibition of hypoxia inducible factor hydroxylases protects against renal ischemia-reperfusion injury. J. Am. Soc. Nephrol. 2008; 19:39–46. [PubMed: 18178798]
35. Kim I, Mogford JE, Witschi C, Nafissi M, Mustoe TA. Inhibition of prolyl 4-hydroxylase reduces scar hypertrophy in a rabbit model of cutaneous scarring. Wound Repair Regen. 2003; 11:368–372. [PubMed: 12950641]
36. Elson DA, Ryan HE, Snow JW, Johnson R, Arbeit JM. Coordinate up-regulation of hypoxia inducible factor (HIF)-1α and HIF-1 target genes during multi-stage epidermal carcinogenesis and wound healing. Cancer Res. 2000; 60:6189–6195. [PubMed: 11085544]
37. Botusan IR, Sunkari VG, Savu O, Catrina AI, Grunler J, Lindberg S, Pereira T, Yla-Herttuala S, Poellinger L, Brismar K, Catrina SB. Stabilization of HIF-1α is critical to improve wound healing in diabetic mice. Proc. Natl. Acad. Sci. U.S.A. 2008; 105:19426–19431. [PubMed: 19057015]
38. Thangarajah H, Yao DC, Chang EI, Shi YB, Jazayeri L, Vial IN, Galiano RD, Du XL, Grogan R, Galvez MG, Januszyk M, Brownlee M, Gurtner GC. The molecular basis for impaired hypoxia-induced VEGF expression in diabetic tissues. Proc. Natl. Acad. Sci. U.S.A. 2009; 106:13505–13510. [PubMed: 19666581]
39. Strehin I, Gourevitch D, Zhang Y, Heber-Katz E, Messersmith PB. Hydrogels formed by oxo-ester mediated native chemical ligation. Biomater. Sci. 2013; 1:603–613. [PubMed: 23894696]
40. Banerji B, Conejo-Garcia A, McNeill LA, McDonough MA, Buck MR, Hewitson KS, Oldham NJ, Schofield CJ. The inhibition of factor inhibiting hypoxia-inducible factor (FIH) by β-oxocarboxylic acids. Chem. Commun. 2005:5438–5440.
41. Safran M, Kim WY, O'Connell F, Flippin L, Gunzler V, Horner JW, Depinho RA, Kaelin WG Jr. Mouse model for noninvasive imaging of HIF prolyl hydroxylase activity: Assessment of an oral agent that stimulates erythropoietin production. Proc. Natl. Acad. Sci. U.S.A. 2006; 103:105–110. [PubMed: 16373502]
42. Blankenhorn EP, Troutman S, Clark LD, Zhang XM, Chen P, Heber-Katz E. Sexually dimorphic genes regulate healing and regeneration in MRL mice. Mamm. Genome. 2003; 14:250–260. [PubMed: 12682777]
43. Repesh LA, Oberpriller JC. Ultrastructural studies on migrating epidermal cells during the wound healing stage of regeneration in the adult newt, Notophthalmus viridescens. Am. J. Anat. 1980; 159:187–208. [PubMed: 6160761]
44. Cheverud JM, Lawson HA, Bouckaert K, Kossenkov A, Showe L, Cort L, Blankenhorn EP, Bedelbaeva K, Gourevitch D, Zhang Y, Heber-Katz E. Fine-mapping quantitative trait loci affecting murine external ear tissue regeneration in the LG/J by SM/J advanced intercross line. Heredity. 2014; 112:508–518. [PubMed: 24569637]
45. Krag M, Knapp D, Nacu E, Khattak S, Maden M, Epperlein H, Henning H, Tanaka EM. Cells keep a memory of their tissue origin during axolotl limb regeneration. Nature. 2009; 460:60–65. [PubMed: 19571878]
46. Vinarsky V, Atkinson DL, Stevenson TJ, Keating MT, Odelberg SJ. Normal newt limb regeneration requires matrix metalloproteinase function. Dev. Biol. 2005; 279:86–98. [PubMed: 15708560]
47. Santosh N, Windsor LJ, Mahmoudi BS, Li B, Zhang W, Chernoff EA, Rao N, Stocum DL, Song F. Matrix metalloproteinase expression during blastema formation in regeneration-competent versus regeneration-deficient amphibian limbs. Dev. Dyn. 2011; 240:1127–1141. [PubMed: 21128310]
48. Globus M, Vethamany-Globus S, Lee YC. Effect of apical epidermal cap on mitotic cycle and cartilage differentiation in regeneration blastemata in the newt, Notophthalmus viridescens. Dev. Biol. 1980; 75:358–372. [PubMed: 7372003]
49. Stocum DL, Crawford K. Use of retinoids to analyze the cellular basis of positional memory in regenerating amphibian limbs. Biochem. Cell Biol. 1987; 65:750–761. [PubMed: 3325080]
50. Stocum DL. The role of peripheral nerves in urodele limb regeneration. Eur. J. Neurosci. 2011; 34:908–916. [PubMed: 21929624]

51. Okuse T, Chiba T, Katsuumi I, Imai K. Differential expression and localization of WNTs in an animal model of skin wound healing. Wound Repair Regen. 2005; 13:491–497. [PubMed: 16176457]
52. Nomachi A, Nishita M, Inaba D, Enomoto M, Hamasaki M, Minami Y. Receptor tyrosine kinase Ror2 mediates Wnt5a-induced polarized cell migration by activating c-Jun N-terminal kinase via actin-binding protein filamin A. J. Biol. Chem. 2008; 283:27973–27981. [PubMed: 18667433]
53. O'Connell MP, Marchbank K, Webster MR, Valiga AA, Kaur A, Vultur A, Li L, Herlyn M, Villanueva J, Liu Q, Yin X, Widura S, Nelson J, Ruiz N, Camilli TC, Indig FE, Flaherty KT, Wargo JA, Frederick DT, Cooper ZA, Nair S, Amaravadi RK, Schuchter LM, Karakousis GC, Xu W, Xu X, Weeraratna AT. Hypoxia induces phenotypic plasticity and therapy resistance in melanoma via the tyrosine kinase receptors ROR1 and ROR2. Cancer Discov. 2013; 3:1378–1393. [PubMed: 24104062]
54. Mitsui K, Tokuzawa Y, Itoh H, Segawa K, Murakami M, Takahashi K, Maruyama M, Maeda M, Yamanaka S. The homeoprotein Nanog is required for maintenance of pluripotency in mouse epiblast and ES cells. Cell. 2003; 113:631–642. [PubMed: 12787504]
55. Niwa H, Miyazaki J, Smith AG. Quantitative expression of Oct-3/4 defines differentiation, dedifferentiation or self-renewal of ES cells. Nat. Genet. 2000; 24:372–376. [PubMed: 10742100]
56. Dunwoodie SL. The role of hypoxia in development of the mammalian embryo. Dev. Cell. 2009; 17:755–773. [PubMed: 20059947]
57. Mohyeldin A, Garzon-Muvdi T, Quinones-Hinojosa A. Oxygen in stem cell biology: A critical component of the stem cell niche. Cell Stem Cell. 2010; 7:150–161. [PubMed: 20682444]
58. Mathieu J, Zhang Z, Zhou W, Wang AJ, Heddleston JM, Pinna CM, Hubaud A, Stadler B, Choi M, Bar M, Tewari M, Liu A, Vessella R, Rostomily R, Born D, Horwitz M, Ware C, Blau CA, Cleary MA, Rich JN, Ruohola-Baker H. HIF induces human embryonic stem cell markers in cancer cells. Cancer Res. 2011; 71:4640–4652. [PubMed: 21712410]
59. Shyh-Chang N, Daley GQ, Cantley LC. Stem cell metabolism in tissue development and aging. Development. 2013; 140:2535–2547. [PubMed: 23715547]
60. Simsek T, Kocabas F, Zheng J, Deberardinis RJ, Mahmoud AI, Olson EN, Schneider JW, Zhang CC, Sadek HA. The distinct metabolic profile of hematopoietic stem cells reflects their location in a hypoxic niche. Cell Stem Cell. 2010; 7:380–390. [PubMed: 20804973]
61. Schmidt, AJ. Cellular Biology of Vertebrate Regeneration and Repair. University of Chicago Press; Chicago: 1968. Metabolites and metabolism in repair and regeneration; p. 121-240.
62. Rao N, Song F, Jhamb D, Wang M, Milner DJ, Price NM, Belecky-Adams TL, Palakal MJ, Cameron JA, Li B, Chen X, Stocum DL. Proteomic analysis of fibroblastema formation in regenerating hind limbs of *Xenopus laevis* froglets and comparison to axolotls. BMC Dev. Biol. 2014; 14:32. [PubMed: 25063185]
63. Hunt TK, Aslam RS, Beckert S, Wagner S, Ghani QP, Hussain MZ, Roy S, Sen CK. Aerobically derived lactate stimulates revascularization and tissue repair via redox mechanisms. Antioxid. Redox Signal. 2007; 9:1115–1124. [PubMed: 17567242]
64. Covello KL, Kehler J, Yu H, Gordan JD, Arsham AM, Hu CJ, Labosky PA, Simon MC, Keith B. HIF-2α regulates Oct-4: Effects of hypoxia on stem cell function, embryonic development, and tumor growth. Genes Dev. 2006; 20:557–570. [PubMed: 16510872]
65. Foja S, Jung M, Harwardt B, Riemann D, Pelz-Ackermann O, Schroeder IS. Hypoxia supports reprogramming of mesenchymal stromal cells via induction of embryonic stem cell-specific microRNA-302 cluster and pluripotency-associated genes. Cell. Reprogram. 2013; 15:68–79. [PubMed: 23256541]
66. Rosenbloom J, Harsch M, Jimenez S. Hydroxyproline content determines the denaturation temperature of chick tendon collagen. Arch. Biochem. Biophys. 1973; 158:478–484. [PubMed: 4592982]
67. Hanauske-Abel HM. Prolyl 4-hydroxylase, a target enzyme for drug development. Design of suppressive agents and the in vitro effects of inhibitors and proinhibitors. J. Hepatol. 1991; 13(Suppl. 3):S8–S15. [PubMed: 1667671]

68. Kroening S, Neubauer E, Wessel J, Wiesener M, Goppelt-Struebe M. Hypoxia interferes with connective tissue growth factor (CTGF) gene expression in human proximal tubular cell lines. Nephrol. Dial. Transplant. 2009; 24:3319–3325. [PubMed: 19549692]
69. Erler JT, Bennewith KL, Cox TR, Lang G, Bird D, Koong A, Le QT, Giaccia AJ. Hypoxia-induced lysyl oxidase is a critical mediator of bone marrow cell recruitment to form the premetastatic niche. Cancer Cell. 2009; 15:35–44. [PubMed: 19111879]
70. Gilkes DM, Bajpai S, Chaturvedi P, Wirtz D, Semenza GL. Hypoxia-inducible factor 1 (HIF-1) promotes extracellular matrix remodeling under hypoxic conditions by inducing *P4HA1*, *P4HA2*, and *PLOD2* expression in fibroblasts. J. Biol. Chem. 2013; 288:10819–10829. [PubMed: 23423382]
71. Luo G, D'Souza R, Hogue D, Karsenty G. The matrix Gla protein gene is a marker of the chondrogenesis cell lineage during mouse development. J. Bone Miner. Res. 1995; 10:325–334. [PubMed: 7754814]
72. Tuckermann JP, Pittois K, Partridge NC, Merregaert J, Angel P. Collagenase-3 (MMP-13) and integral membrane protein 2a (*Itm2a*) are marker genes of chondrogenic/osteoblastic cells in bone formation: Sequential temporal, and spatial expression of Itm2a, alkaline phosphatase, MMP-13, and osteocalcin in the mouse. J. Bone Miner. Res. 2000; 15:1257–1265. [PubMed: 10893674]
73. van der Weyden L, Wei L, Luo J, Yang X, Birk DE, Adams DJ, Bradley A, Chen Q. Functional knockout of the matrilin-3 gene causes premature chondrocyte maturation to hypertrophy and increases bone mineral density and osteoarthritis. Am. J. Pathol. 2006; 169:515–527. [PubMed: 16877353]
74. Moser M, Bosserhoff AK, Hunziker EB, Sandell L, Fässler R, Buettner R. Ultrastructural cartilage abnormalities in MIA/CD-RAP-deficient mice. Mol. Cell. Biol. 2002; 22:1438–1445. [PubMed: 11839810]
75. Heinegård D. Proteoglycans and more—From molecules to biology. Int. J. Exp. Pathol. 2009; 90:575–586. [PubMed: 19958398]
76. Han L, Grodzinsky AJ, Ortiz C. Nanomechanics of the cartilage extracellular matrix. Annu. Rev. Mater. Res. 2011; 41:133–168. [PubMed: 22792042]
77. Ohyama M, Terunuma A, Tock CL, Radonovich MF, Pise-Masison CA, Hopping SB, Brady JN, Udey MC, Vogel JC. Characterization and isolation of stem cell-enriched human hair follicle bulge cells. J. Clin. Invest. 2006; 116:249–260. [PubMed: 16395407]
78. Ito M, Kizawa K. Expression of calcium-binding S100 proteins A4 and A6 in regions of the epithelial sac associated with the onset of hair follicle regeneration. J. Invest. Dermatol. 2001; 116:956–963. [PubMed: 11407987]
79. Snyder HR, Freier HE. Some substituted 1,10-phenanthrolines. J. Am. Chem. Soc. 1946; 68:1320–1322. [PubMed: 20990996]
80. Cramer T, Yamanishi Y, Clausen BE, Forster I, Pawlinski R, Mackman N, Haase VH, Jaenisch R, Corr M, Nizet V, Firestein GS, Gerber HP, Ferrara N, Johnson RS. HIF-1α is essential for myeloid cell-mediated inflammation. Cell. 2003; 112:645–657. [PubMed: 12628185]
81. Jones MK, Szabo IL, Kawanaka H, Husain SS, Tarnawski AS. Von Hippel Lindau tumor suppressor and HIF-1α: New targets of NSAID inhibition of hypoxia-induced angiogenesis. FASEB J. 2002; 16:264–266. [PubMed: 11772947]
82. Palayoor ST, Tofilon PJ, Coleman CN. Ibuprofen-mediated reduction of hypoxiainducible factors HIF-1α and HIF-2α in prostate cancer cells. Clin. Cancer Res. 2003; 9:3150–3157. [PubMed: 12912967]

One-sentence summary

The capacity for regeneration can be elicited in adult mice by drug-induced stabilization of hypoxia-inducible factor -1α (HIF-1α) protein.

Editor'S Summary

Driving regeneration in mice

The MRL mouse is capable of regenerating injured tissues, making it a rare exception among mammals. The markedly increased expression of hypoxia-inducible factor-1α (HIF-1α) found both before and after injury in the MRL mouse could account for some of the cellular, molecular, and metabolic hallmarks of regeneration. To test this hypothesis, Zhang *et al.* used a drug in a slow-release hydrogel formulation to up-regulate HIF-1α protein expression after ear hole punch injury in adult Swiss Webster mice that do not normally show regeneration. The authors observed ear hole healing with closure and a pattern of expression of cellular markers similar to that observed in MRL mice during regeneration in response to injury. A small interfering RNA against *Hif1a* blocked regeneration in both untreated MRL mice and drug-treated Swiss Webster mice, showing that HIF-1α is a central driver of regeneration in mice.

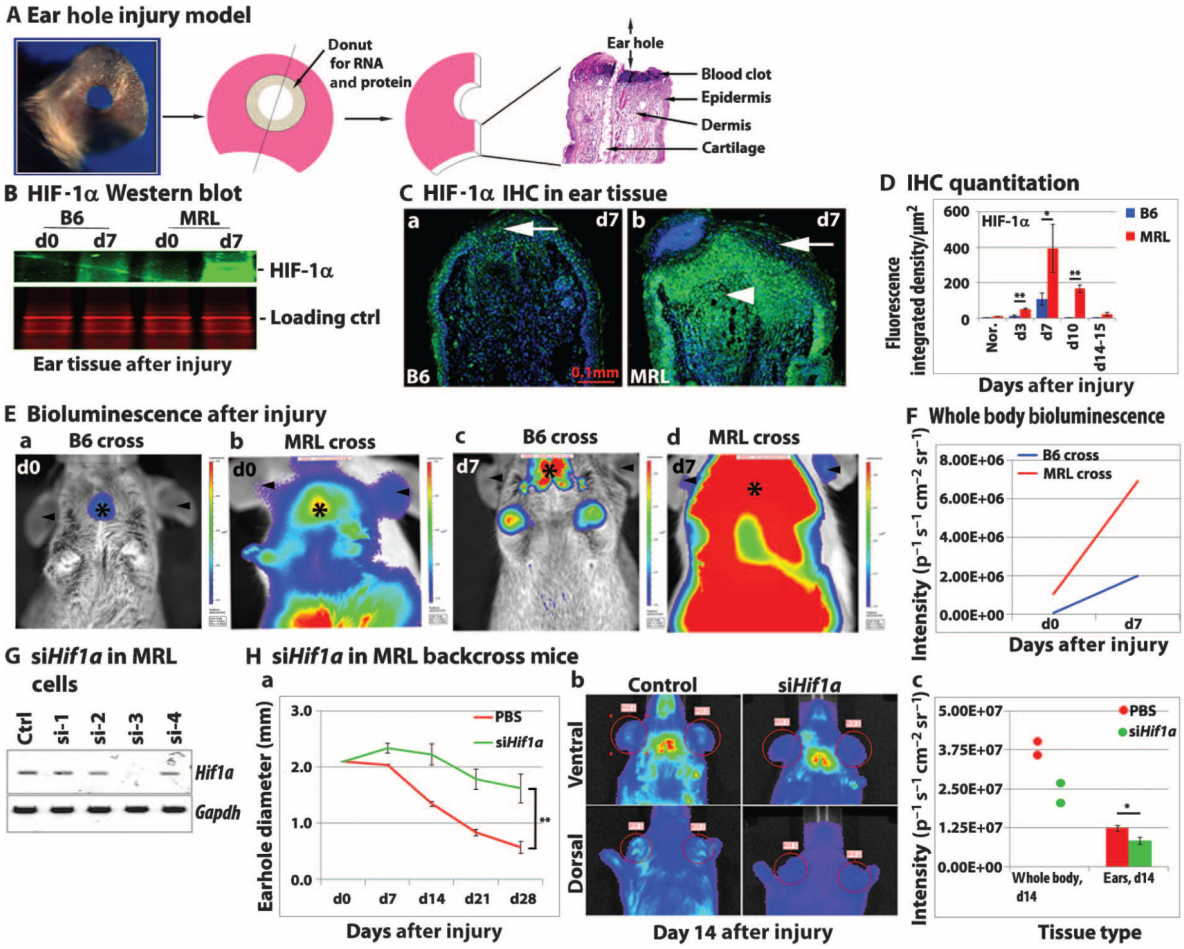

Fig. 1. HIF-1α protein is required for the regenerative response of the MRL mouse

(**A**) Schematic shows ear punch injury, and images show resulting histological sections and processed tissue samples. (**B** to **F**) HIF-1α protein expression in MRL and B6 mice before and after ear wounding. (B) Pooled ear hole donuts (n = 4) were processed for HIF-1α Western blot analysis with Coomassie blue–stained protein (seen as red with the Odyssey Classic Infrared Imaging System) as a loading control; N = 2 experiments. (C) Ear tissue was used for HIF-1α immunostaining (green; arrows show epidermal HIF-1α expression and arrowheads show dermal HIF-1α expression). Scale bar, 0.1 mm. (D) Multiple ear tissue samples for each time point after injury (n = 3 to 7 samples, N = 2 experiments) were quantitatively analyzed for MRL and B6 mice on day 7 (*P < 0.05) and on days 3 and 10 (**P < 0.01). (E) Further confirmation of HIF-1α expression was carried out in MRL and B6 mice backcrossed (BC4) to transgenic HIF-1α peptide–luciferase reporter mice. MRL.HIF-luc and B6.HIF-luc mice showed luciferase activity as measured by bioluminescence. This is seen as red for the highest bioluminescent activity and blue for the lowest activity. Arrowheads indicate ear bioluminescence; asterisks indicate body bioluminescence. (F) IVIS (in vivo imaging system, Perkin Elmer), a small animal bioluminescence detector, measured photon number in steradians (a unit of measure based on a solid angle) on days 0 and 7 in the healing ear and whole MRL cross mouse (red) and in the wounded ear and whole B6 cross mouse (blue); data are expressed as photons per

second per square centimeter per steradian (p^{-1} s^{-1} cm^{-2} sr^{-1}). Panel (E) shows one representative mouse per group as an example of a set of multiple experiments with $n = 5$ mice per group. In (F), the total number of photons detected in each of the mice from (E) is shown. (**G** and **H**) HIF-1α expression is required during MRL ear hole closure. (G) Treatment with *Hif1a* siRNA (si*Hif1a*) blocked *Hif1a* mRNA expression in vitro in MRL mouse ear fibroblasts ($n = 3$ replicates); *Gapdh* is the loading control ($N = 2$ experiments). (H) Treatment of MRL.HIF-luc mice after ear punching with si*Hif1a*_3 in vivo. Mice were injected subcutaneously with either JETPEI-si*Hif1a*_3 mixture at days 0 to 20 after injury (15 μg per mouse; green) or phosphate-buffered saline (PBS; red). (a) Ear hole closure was blocked on day 28; $^{**}P < 0.001$, Student's *t* test ($n = 4$ ears per group, $N = 2$ experiments). (b) HIF-1α was determined by bioluminescence (dorsal and ventral) in reporter mice treated with si*Hif1a*_3. (c) Number of photons detected on day 14 in the whole mouse ($n = 2$) or injured ear; $^{*}P < 0.05$, Student's *t* test ($n = 4$ ear samples per group) for si*Hif1a*_3 compared to control ($N = 2$ experiments).

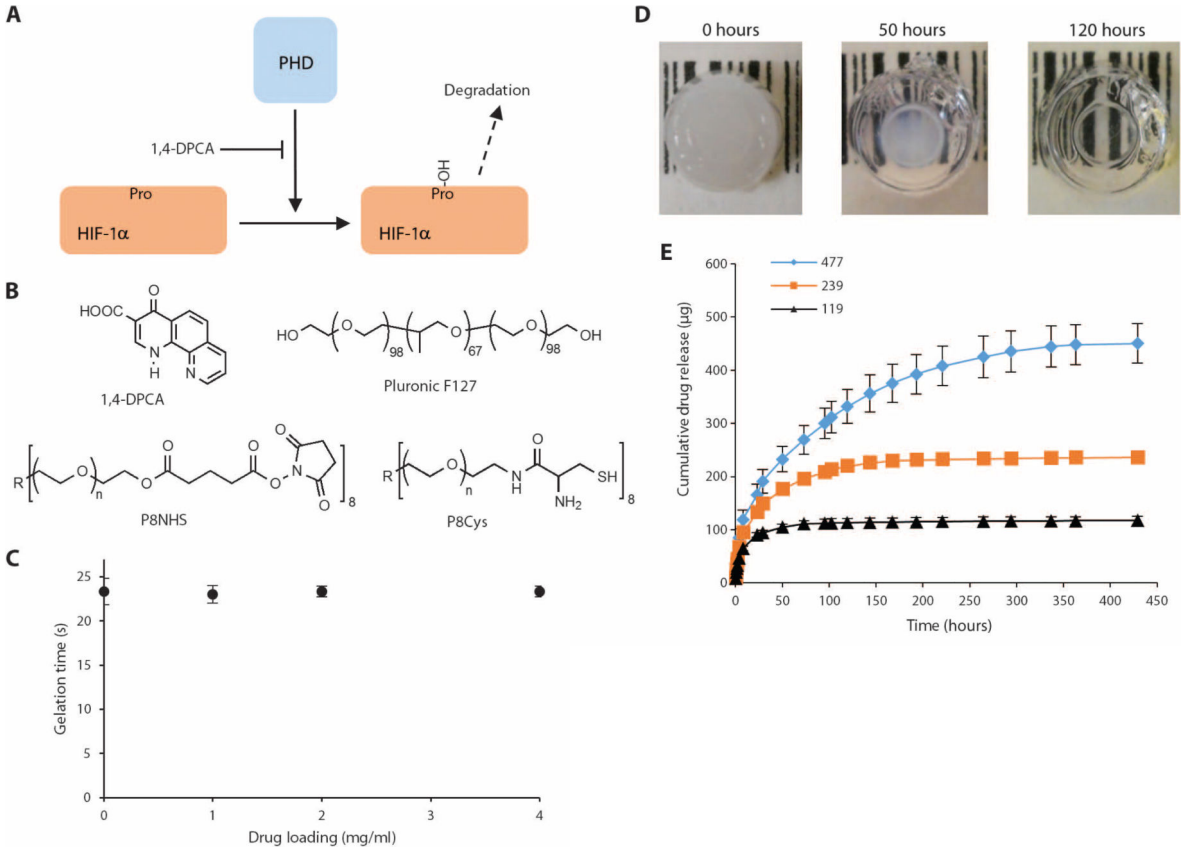

Fig. 2. The drug 1,4-DPCA, an inhibitor of PHDs, is encapsulated in an injectable polymer hydrogel and released over several days

(**A**) Diagram showing that blockade of PHDs by 1,4-DPCA slows degradation of HIF-1α. (**B**) Chemical structures of the drug delivery components include the drug1,4-DPCA; Pluronic F127, which coats drug crystals; and P8NHS and P8Cys, which react to form the polymer hydrogel that contains the drug. (**C**) The presence of drug microcrystals does not interfere with the gelation kinetics of the hydrogel. (**D**) The drug was encapsulated in the hydrogel, yielding a white, opaque cylindrical hydrogel (left), which when incubated with PBS released the drug, leaving behind a clear hydrogel (right). (**E**) In vitro experiments showed that drug release occurred over several days for hydrogels containing 119 to 477 μg of the 1,4-DPCA drug. Colored lines represent total drug loading for each formulation. Panels (C) and (E) show data from replicate samples (n = 3).

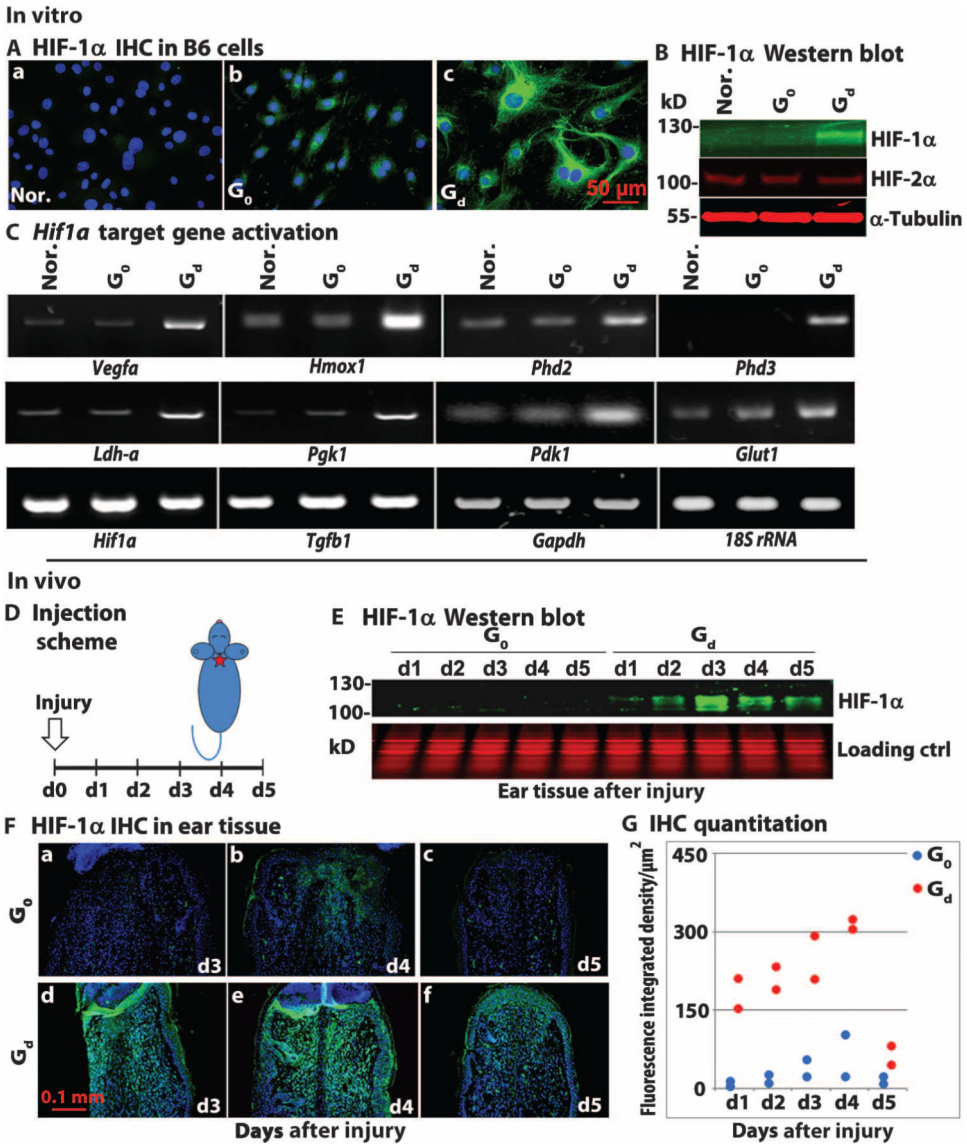

Fig. 3. 1,4-DPCA drug/gel stabilizes HIF-1α, but not HIF-2α, in vitro and in vivo

(**A**) Ear fibroblasts from B6 mice were cultured with normal medium (Nor.), gel alone (G_0), or drug (2 mg/ml)/gel (G_d) in 100-μl total volume, which formed a solid disc in 24-well plates. Addition of 1,4-DPCA drug/gel (G_d) induced HIF-1α protein expression as determined by immunostaining (green, panel c). Scale bar, 50 μm. (**B**) Cell lysates (n = 3 per lane) from (A) were used for Western blot analysis for HIF-1α protein (green) and HIF-2α (red) compared to control protein α-tubulin (red) (N = 4). (**C**) Activation of HIF-1α target gene transcription. RT-PCR was used to analyze mRNA extracted from drug-treated mouse B6 cells (n = 3) from (A). The expression of multiple genes was increased by the 1,4 DPCA/gel treatment, including proangiogenic target genes *Vegf* and *Hmox1*, and proglycolytic targets *Ldh-a*, *Pgk*, *Pdk1*, and *Glut1*. *Gapdh* and 18*S* ribosomal RNA were used as internal controls for all RT-PCR reactions (N = 3). (**D** to **G**) Swiss Webster mice were treated with a single injection of drug/gel on day 0, the day of injury, and ear tissue was harvested everyday for 5 days and was tested for HIF-1α up-regulation. (D) Schematic

illustrates the in vivo treatment schedule. Swiss Webster mice were ear-punched and injected several hours later in the back of the neck with either gel alone (G_0) or drug/gel (G_d). Ear donut tissue was collected for protein and immunohistochemical (IHC) analysis on days 1 to 5. In (E), hole donuts ($n = 6$) were processed, and Western blot analysis was carried out using antibody to HIF-1α (green) and Coomassie-stained samples as loading controls (red) ($N = 3$). (F) Immunostaining of ear tissue with anti–HIF-1α antibody (green) and 4′,6-diamidino-2-phenylindole (DAPI) counterstain (blue). (G) Immunohistochemical quantitation for G_0 (blue) and G_d (red) tissue showed nonoverlapping differences at all time points ($n = 2$ per treatment group, $N = 2$ experiments).

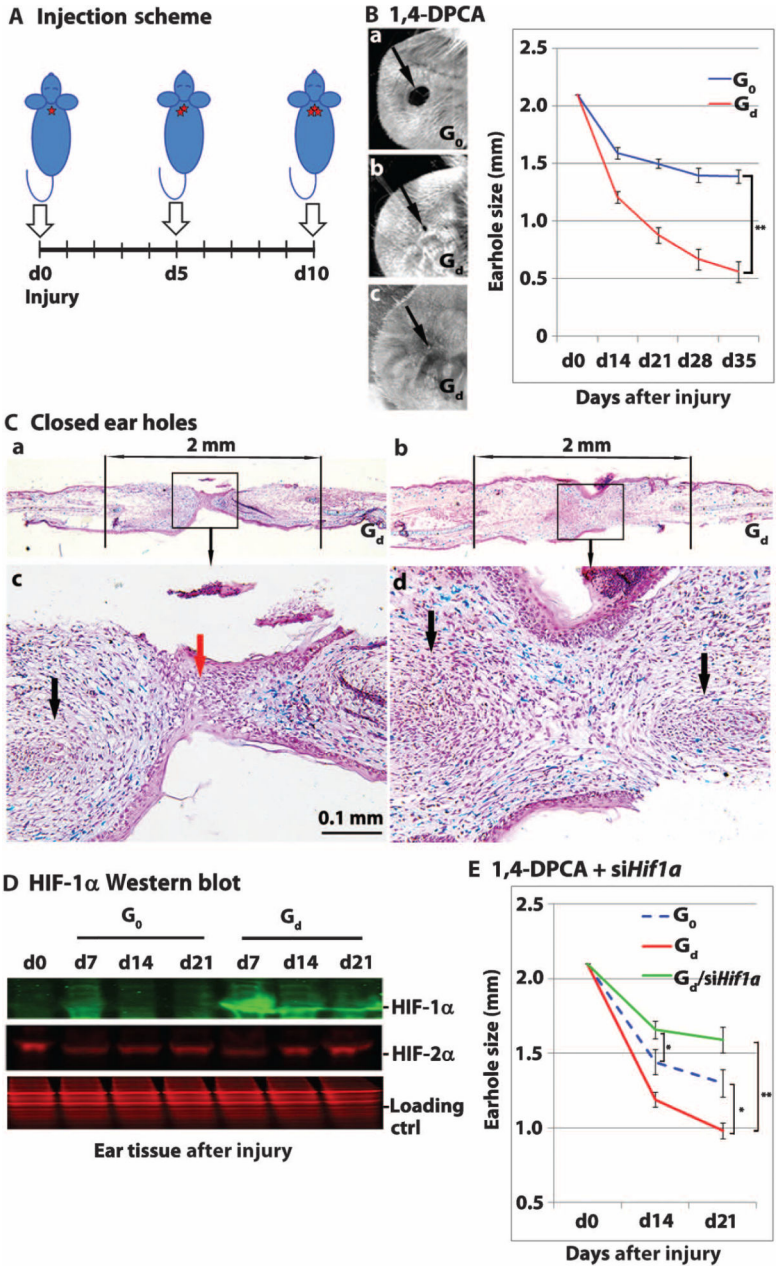

Fig. 4. Sequential injections of 1,4-DPCA drug/gel into mice at 5-day intervals promote ear hole closure

(**A**) Injection scheme for Swiss Webster mice ear-punched on day 0 and injected with drug/gel on days 0, 5, and 10 into separate locations at the base of the neck (one site every 5 days, indicated by arrows). (**B**) Mice were injected with either gel alone [G_0; drug (0 mg/ml)/gel, blue line] or drug/gel [G_d; drug (2 mg/ml)/gel, red line] and were followed for 35 days. Results of wound healing with three injections of drug (2 mg/ml)/gel were compared to G_0 on day 35 (**$P < 0.0001$; Student's t test; $n = 10$ ears, $N = 4$). Images on the left are representative of day 35 ear pinnae (arrows point to ear holes) (a, 0 mg drug/gel; b and c, 2 mg drug/gel). (**C**) Histological analysis of Alcian blue–stained day 35 ear tissue treated with 1,4-DPCA/gel (a and b) with the 2-mm area of the original hole indicated; (c

and d) higher magnification ($n = 2$). Areas of cartilaginous condensation are shown (black arrows); blue staining indicates the presence of proteoglycans. Panel (c) shows a less complete closure where epithelial cells (red arrow) still persist in the new bridge region. In panel (d), ear hole closure is more complete with the bridge filled with mesenchymal cells. (**D**) Hole donuts ($n = 6$) from punched ears treated with gel alone (G_0) or drug/gel (G_d) were processed, and Western blot analysis (using the Odyssey Classic Infrared Imaging System) was carried out ($N = 3$) with anti–HIF-1α (green) or anti–HIF-2α (red) antibodies; Coomassie protein staining is the loading control (red). (**E**) Treatment of Swiss Webster mice with drug/gel and si*Hif1a* showed inhibition of ear hole closure at day 21 after injury (green line) compared to mice treated with drug/gel only (red line) (**$P < 0.001$). Drug/gel + si*Hif1a* treatment (green line) compared to gel only (G_0) (blue line) showed differences in inhibition of ear hole closure on day 14 (*$P < 0.05$) but not on day 21 ($P = 0.051$). Comparing ear hole closure in G_0-treated (blue line) and G_d-treated (red line) Swiss Webster mice showed differences at day 21 (*$P < 0.05$; $n = 4$ to 7, $N = 2$). Analysis of variance (ANOVA) statistical analysis was used.

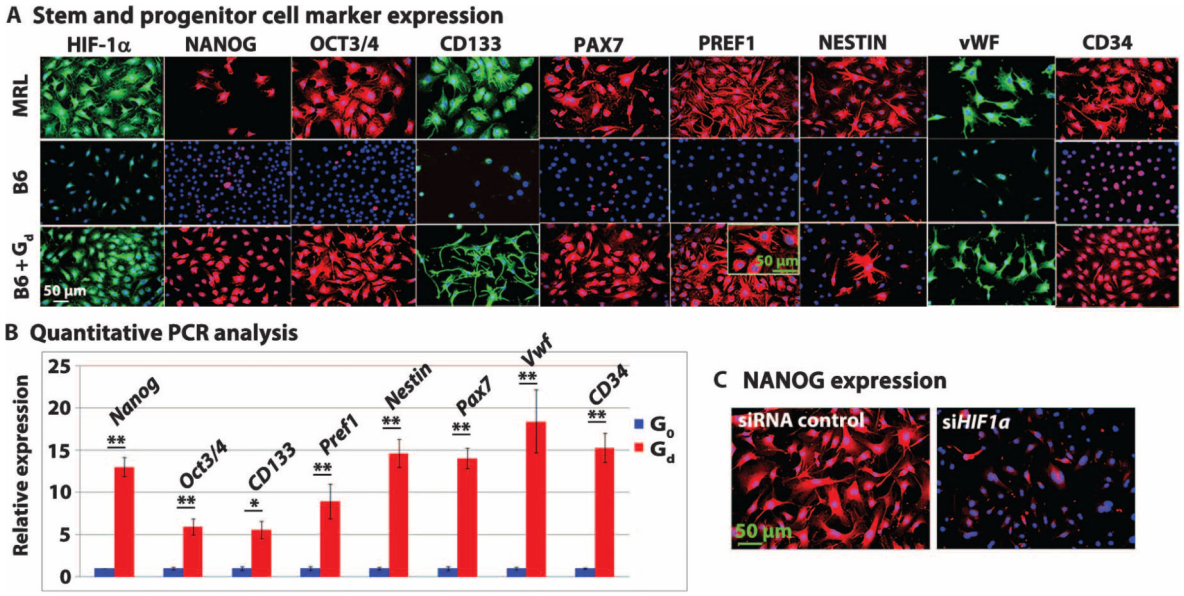

Fig. 5. HIF-1α stabilization by 1,4-DPCA drug/gel induces stem and progenitor cell marker expression in vitro

(**A**) Stem and progenitor cell marker expression. Cultured MRL mouse fibroblasts (top row) and B6 mouse fibroblasts (middle row) were grown on coverslips and immunostained with antibodies against HIF-1α, NANOG, OCT3/4, CD133, PAX7, PREF1 (DLK1), NESTIN, von Willebrand factor (vWF), and CD34. B6 mouse fibroblasts were cultured with drug (2 mg/ml)/gel (B6 + G_d,; bottom row) for 24 hours (n = 5 to 10 fields per coverslip, N = 3). (**B**) Quantitative PCR analysis. Results of qPCR were consistent with immunohistochemistry showing marked changes in mRNA expression for all stem cell markers in the drug-treated cells compared to untreated cells (n = 3, N = 3, see table S6; *P < 0.05, **P < 0.01, Student's t test). (**C**) NANOG expression. MRL mouse fibroblasts (n = 3 coverslips per group) were treated with either siRNA control (left) or si*Hif1a* (right) for 48 hours and were immunostained with anti-NANOG antibody (N = 2). All scale bars, 50 μm.

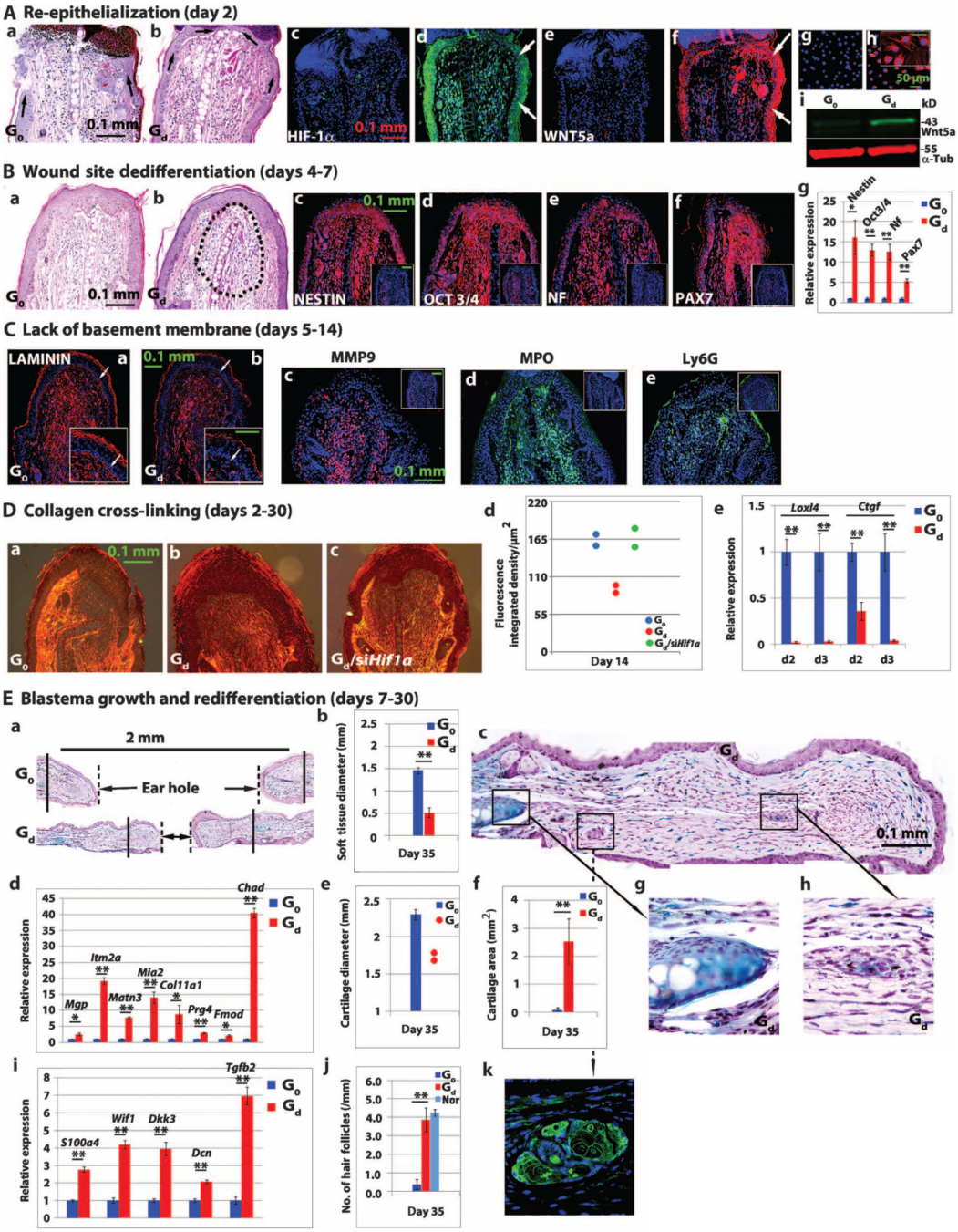

Fig. 6. Major steps in tissue regeneration

(**A**) Reepithelialization of punched ear tissue (n = 4 per group) was seen on day 2 after punch hole injury of Swiss Webster mice. Ear tissue from mice treated with gel only (G_0) or drug/gel (G_d) was stained with hematoxylin and eosin (H&E); black arrows show incomplete (a) versus complete epidermis (b). Immunostaining of ear tissue was done for HIF-1α expression (c and d) and WNT5a expression (e and f) after G_0 (c and e) or G_d (d and f) treatment; white arrows indicate epidermis. Immunohistochemistry of WNT5a protein expression in vitro without (g) or with (h) 1,4-DPCA drug/gel treatment; (i) Western blot

analysis of pooled tissue (n = 3, N = 2). (**B**) H&E-immunostained sections of mouse ear tissue (day 4 after injury) show dedifferentiation in the area of the G_d-treated wound site (b, dashed black lines). G_d- and G_0-treated ear tissues were immunostained for NESTIN, OCT3/4, neurofilament (NF), and PAX7 (c to f) (n = 4). G_0 controls are shown in insets. Results of qPCR for these same genes are seen in (g) (n = 3, N = 3; *P < 0.05, **P < 0.01, Student's t test). (**C**) Ear tissue from G_d-treated versus G_0-treated mice was immunostained to show laminin expression and basement membrane breakdown (white arrows, a and b, inset). (c to e) Expression of MMP9, MPO, and Ly6G protein in G_d-treated versus G_0-treated (insets) mice (n = 4, N = 3). (A to C) Blue is DAPI counterstain; red or green color shows specific immunostaining. (**D**) Picrosirius red staining analysis shows day 14 collagen cross-linking in ear tissue from Swiss Webster mice treated with gel only G_0 (a), drug/gel G_d (b), or G_d + si*Hif1a* (c). Quantitated polarized light analysis (d) shows nonoverlapping differences between G_0-treated and G_d-treated ear tissue and between G_d-treated and G_d + si*Hif1a*–treated ear tissue (n = 2). (e) qPCR results show early (days 2 to 3 after injury) *Loxl4* and *Ctgf* expression in G_d- and G_0-treated ear tissue samples (n = 3 per group, N = 3; **P < 0.01, Student's t test). (**E**) Blastema growth and redifferentiation into cartilage and hair follicles was seen in Swiss Webster ear tissue after G_d treatment. (a) Low-magnification histological image of ear hole tissue stained with Alcian blue shows chondrogenesis in G_d-treated but not in G_0-treated ear tissue. Solid vertical lines indicate ends of cartilage; broken lines show soft tissue borders. (b) Quantitation of soft tissue ear hole diameter at day 35 after injury. (c) A magnified image of G_d-treated mouse ear tissue indicates two new areas of chondrogenesis (g and h) and new hair follicles (k). Results of qPCR show up-regulated chondrogenesis-associated (d) and hair follicle–associated (i) genes on day 21 after injury in G_d-treated but not in G_0-treated mouse ear tissue (*P < 0.05, **P < 0.01, Student's t test; n = 3, N = 3). Cartilage hole diameter (e) and cartilage area (f) (a histomorphometric measurement of Alcian blue staining in new growth area) were significantly different between G_d-treated and G_0-treated mouse ear tissue (**P < 0.01, Student's t test; n = 4 to 6 ears). (j) Number of keratin 14–positive hair follicles in G_d-treated mouse ear tissue compared to G_o-treated and normal mouse ear tissue. **P < 0.0001, ANOVA (n = 4 ears). Scale bars, 0.1 mm for all panels except for panel (Ah) (50 μm).